

Support-induced promotional effects on the activity of automotive exhaust catalysts:

1. The case of oxidation of light hydrocarbons (C₂H₄)

C. Pliangos, I.V. Yentekakis, V.G. Papadakis, C.G. Vayenas, X.E. Verykios*

Department of Chemical Engineering, University of Patras, Patras GR-26500, Greece

Received 9 December 1996; received in revised form 26 February 1997; accepted 26 February 1997

Abstract

The kinetics of oxidation of a light hydrocarbon (C₂H₄) were studied on catalysts comprising of combinations of one of three metals, Pt, Pd or Rh supported on five different supports, that is, SiO₂, γ-Al₂O₃, ZrO₂ (8% Y₂O₃), TiO₂ or TiO₂ (W⁶⁺). Significant variation of turnover frequency with the carrier was observed, which cannot be explained by structure sensitivity considerations and is attributed to interactions between the metal crystallites and the carrier. The catalytic activity of these metal-support combinations was investigated over a wide range of partial pressures of ethylene and oxygen. In a separate set of experiments, the kinetics of C₂H₄ oxidation were also investigated on polycrystalline Rh films interfaced with ZrO₂ (8 mol% Y₂O₃) solid electrolyte in a galvanic cell of the type: C₂H₄, O₂, Rh/YSZ/Pt, air, during regular open-circuit conditions as well as under Non-Faradic Electrochemical Modification of Catalytic Activity (NEMCA), that is, closed-circuit conditions. Up to 100-fold increase in catalytic activity was observed by supplying O²⁻ ions to the catalyst surface via positive potential application to the catalyst. The observed kinetic behavior upon increasing catalyst potential parallels qualitatively the observed alteration of turnover frequency with variation of the support of the Rh crystallites. © 1997 Elsevier Science B.V.

Keywords: Promotion; Catalytic converter; Ethylene oxidation; Platinum; Palladium; Rhodium; Electrochemical promotion

1. Introduction

Rhodium, platinum and palladium are the main constituents of three-way automotive exhaust catalysts and the catalytic chemistry related to the interactions of O₂, NO_x, CO and light hydrocarbons has been the focal point of numerous investigations [1–9] and review articles [10–13] over the past two decades. Due to the high cost of the noble metals used in three-way catalysts, reduction in the required amounts in

automotive exhaust catalytic converters, via appropriate promotion of their catalytic properties, would be highly desirable.

It has often been demonstrated that the effects of the support on the performance of metal catalysts can be very significant. A specific kind of metal–support interaction was first established by the early work of Schwab [14] and Solymosi [15] who attributed these phenomena to changes in the electronic state of the metal via electronic-type interactions with the carrier. In recent years, interactions of Group VIII metals with TiO₂ supports induced by high-tempera-

*Corresponding author.

ture reduction were described under the concept of SMSI [16] and were shown to originate from migration of TiO_x species onto the surface of the metal crystallites [17], and possibly from an electronic factor operating concomitantly [18]. More recently it has been found that incorporation of altrivalent cations into the crystal structure of semiconductive carriers can play an important role in defining the catalytic properties of the supported metal crystallites [19–23]. According to proposed explanations, these effects are due to electronic interactions at the metal–support interface caused by the different Fermi levels of the two solids in contact [24].

Significant research efforts have been applied over the past few decades toward the development of more efficient automotive emission-control catalysts. However, limited studies of the effects of the carrier on the chemistry of three-way catalytic converters have appeared in the literature. In this respect, Metcalfe and Sundaresan [25] reported that Y_2O_3 -stabilized ZrO_2 (YSZ) is a better support of Rh than Al_2O_3 for the CO/O_2 and CO/NO reactions, and, more recently, Oh [26] found that a modified $\text{Rh}/\text{CeO}_2/\text{Al}_2\text{O}_3$ catalyst results in higher activity for NO reduction by CO than the $\text{Rh}/\text{Al}_2\text{O}_3$ catalyst. Baiker and coworkers have also found enhanced catalytic properties of supported metal/ ZrO_2 catalysts [27–31]. The catalytic properties of several metals such as Pd, Cu, Fe and Ni, dispersed on ZrO_2 have been investigated for a variety of reactions such as NH_3 synthesis [27,28], CO oxidation [30], NO reduction [31] and CO, CO_2 and hydrocarbons hydrogenation [29,31].

During the last few years it has been found [32,33] that solid electrolytes such as ZrO_2 (8% Y_2O_3), an O^{2-} ion conductor [33,34], $\beta''\text{-Al}_2\text{O}_3$ a Na^+ ion conductor [35], CaF_2 a F^- ion conductor [36], CsHSO_4 , a H^+ ion conductor [37], and mixed conductors, such as TiO_2 [38] can be used for in situ controlled promotion of the catalytic activity of metal catalysts interfaced with these active supports. This effect, termed NEMCA [32,33] or Electrochemical Promotion in catalysis [39], or in situ controlled promotion [35] has been shown to be due to an electrochemically controlled migration (back-spillover) of promoting ions from the solid electrolyte onto the gas-exposed catalyst surface [40–42], and to the effect of these species on the binding strength of chemisorbed reactants and intermediates [33,41].

Work in this area has been reviewed recently [33,40]. Similar galvanic cells, based on yttria stabilized zirconia (YSZ) solid electrolyte, have also been used in the field of heterogeneous catalysis for the study of the mechanism of several catalytic reactions on metals [43–45] via the technique of solid electrolyte potentiometry (SEP) originally proposed by Wagner [46]. This technique is particularly suitable for the study of oscillatory catalytic reactions [44,45].

The present communication constitutes the first part of an extended investigation of the kinetic behavior of Rh, Pt and Pd dispersed on five different supports, that is, SiO_2 , $\gamma\text{-Al}_2\text{O}_3$, ZrO_2 (8% Y_2O_3), TiO_2 and TiO_2 doped with W^{6+} cations (TiO_2 (W^{6+})) under the three main reactions related with the chemistry of automotive emission control that is, CO oxidation, NO reduction by CO, and oxidation of C_2H_4 (as a model hydrocarbon). In this part, results related to the performance of the above catalysts under C_2H_4 oxidation conditions at atmospheric pressure, in the temperature range of 150 to 500°C, are presented. An additional objective of the present work was to explore the possible relationship between the NEMCA effect [33] and the effect of dopant-induced-metal-support interactions [16,19]. For this purpose, the kinetics of C_2H_4 oxidation were also investigated on polycrystalline Rh films interfaced with ZrO_2 (8 mol% Y_2O_3) solid electrolyte in a galvanic cell of the type C_2H_4 , O_2 , Rh/YSZ/Pt, air, under open-circuit conditions where the SEP technique can be used for the in situ monitoring of oxygen activity on the catalyst surface, as well as under closed circuit conditions where the reaction rate can be promoted via the NEMCA effect.

2. Experimental

2.1. Materials

Rh, Pd and Pt catalysts were prepared by the method of incipient wetness impregnation of the supports with a solution of $\text{Rh}(\text{NO}_3)_2 \cdot 2\text{H}_2\text{O}$, PdCl_2 , H_2PtCl_6 (Alfa Products) respectively. The solution was of appropriate strength so as to yield 0.5 wt% metal loadings. The following powder supports were used: SiO_2 (Altech Associates), TiO_2 (Degussa P25) ZrO_2 (8% Y_2O_3) (Zirconia Sales) and $\gamma\text{-Al}_2\text{O}_3$ (Akzo

Chemicals). W^{6+} -doped TiO_2 was prepared following the procedure which has been described elsewhere [19]. The dopant content was 0.45 at.%. The doped and undoped TiO_2 supports were thermally treated (5 h, $900^\circ C$) while the ZrO_2 (8% Y_2O_3) supports underwent thermal pretreatment at $1500^\circ C$ during production. Details of the preparation procedure of the supported catalysts can be found elsewhere [21]. Before any measurements, the catalysts were reduced in a quartz tube under He flow ($80\text{ cm}^3/\text{min}$) at $250^\circ C$ for 1 h followed by H_2 flow ($80\text{ cm}^3/\text{min}$) at $400^\circ C$ for 1 h.

2.2. Catalyst characterization

The characterization of the catalysts was carried out in a BET apparatus (Accusorb 2100E, Micromeritics) with H_2 chemisorption at 298 K and N_2 and/or Ar physical adsorption at 77 K.

2.3. Apparatus

Catalyst testing was performed in a flow apparatus (Fig. 1) which consists of a feed unit, the reactor and an analysis unit utilizing on-line gas chromatography

and IR spectroscopy, for the analysis of reactants and products. Two types of reactors were used: in the case of supported catalysts, an atmospheric pressure continuous-flow quartz reactor was used. It has a volume of 3 cm^3 and behaves as a continuous-flow stirred tank reactor (CSTR) in the flow range of $10\text{--}500\text{ cm}^3\text{ STP}/\text{min}$, as has been shown by determination of its residence time distribution using the IR CO_2 analyser. The catalyst loading in the reactor was typically about 5 mg.

In the case of NEMCA and SEP experiments, a galvanic cell-reactor of the type of closed flat end tube [33] was used which also behaves as a CST reactor at the feed flow rates used in the present work. The porous Rh catalyst film was deposited on the inside flat bottom of the YSZ tube by applying a thin coating of Engelhard A8826 Rh resinate paste, followed by drying and calcining in air at $850^\circ C$ for 6 h. The outside Pt counter and reference electrodes were deposited by coating Engelhard A 1121 Pt resinate followed by calcination in air at $750^\circ C$ for 1 h. The true surface area of Rh catalyst films was measured by a chemical titration technique described in detail elsewhere [45]. Reactants were Messer Griesheim-certified standards of 10% C_2H_4 in He and 20% O_2 in He.

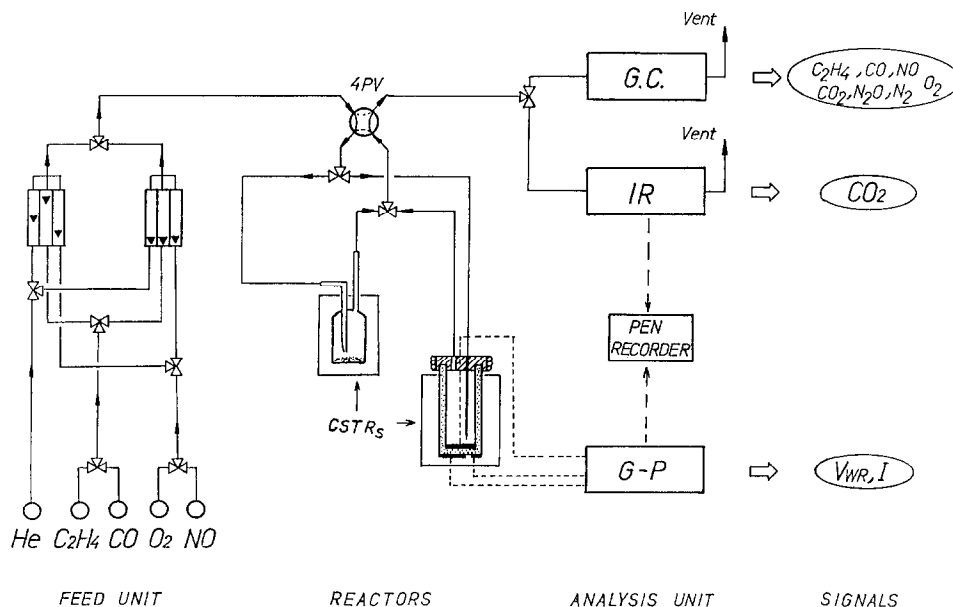


Fig. 1. Schematic representation of the experimental apparatus.

They could be further diluted in ultrapure (99.996%) He (L'Air Liquide).

Rate measurements carried out on both supported or film catalysts were conducted in the kinetic regime. Intraparticle and interparticle diffusional resistances were experimentally eliminated by variation of catalyst particle size and feed flow rate.

3. Results

3.1. Catalyst characterization

The active surface area of fifteen catalysts used in the present study was measured via H_2 chemisorption at 298 K. The hydrogen-to-metal ratio (H/M, M: Rh, Pd or Pt) was calculated assuming a 1 : 1 hydrogen-to-metal stoichiometry. BET surface area of these catalysts was measured with N_2 and/or Ar physical adsorption at 77 K. The results for all catalysts tested are summarized in Table 1.

3.2. Catalytic behavior of supported Rh, Pd and Pt catalysts

The kinetics of C_2H_4 oxidation were investigated in detail over one of the model catalysts (e.g. Rh/ZrO₂ (8% Y₂O₃)) in the temperature range of 150 to 500°C and in the oxygen and ethylene partial pressure range of 0–10 kPa. Only comparative kinetic results at 320°C for all model catalysts are shown here. Fig. 2 shows the effect of oxygen partial pressure, P_{O_2} , on the turnover number, N_{CO_2} , of ethylene oxidation over the five supported Rh catalysts (Table 1) at

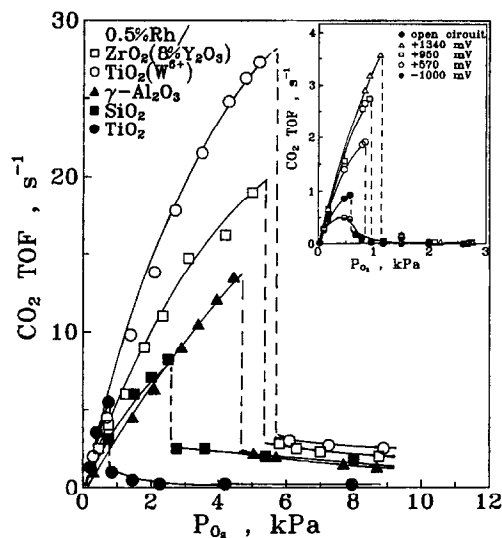


Fig. 2. Effect of partial pressure of oxygen (P_{O_2}) and supports on catalytic turnover rate of Rh catalyst. Insert: Effect of P_{O_2} and catalyst potential on turnover rate of Rh-film catalyst [34]. $P_{C_2H_4} = 3$ kPa, $T = 320^\circ\text{C}$.

constant $P_{C_2H_4}$. The reaction rate over all catalysts behaves as near first-order in P_{O_2} , until a critical P_{O_2} value is reached, hereafter denoted as $P_{O_2}^*$ at which the rate decreases abruptly and subsequently becomes negative-order in oxygen.

Fig. 3 depicts the effect of $P_{C_2H_4}$ on the turnover number of ethylene oxidation over the same model catalysts, at constant P_{O_2} . At low ethylene pressures the rate increases almost linearly with $P_{C_2H_4}$ until a critical value is reached, hereafter denoted as $P_{C_2H_4}^*$ at which the rate increases abruptly to a much higher value and becomes near zero-order in ethylene. The

Table 1
Catalyst characteristics

Catalyst	Support:	Dispersion [H/M] ^a				
		ZrO ₂ (8%Y ₂ O ₃)	TiO ₂	TiO ₂ (4%WO ₃)	γ -Al ₂ O ₃	SiO ₂
Rh		0.44	0.10	0.3	1.0	0.65
Pt		0.44	0.0	1	0.68	0.54
Pd		0.37	0.33	0.33	0.61	0.65
BET surface area (m ² /g) ^b		1.55 ± 0.04	—	—	177.1 ± 1.2	261.7 ± 2.2
BET surface area (m ² /g) ^c		5.2 ± 0.6	0.13 ± 0.02	4.9 ± 0.9	—	—

The metal loading of all fifteen catalysts was 0.5 wt%.

^a H_2 chemisorption at 298 K.

^b N_2 physical adsorption at 77 K.

^c Ar physical adsorption at 77 K.

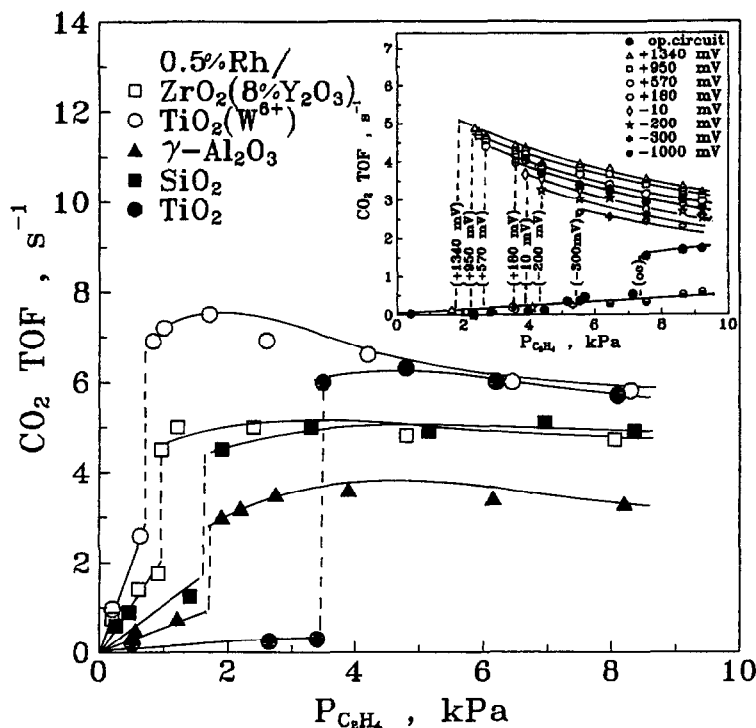


Fig. 3. Effect of partial pressure of ethylene ($P_{C_2H_4}$) and supports on catalytic turnover rate of Rh catalyst. Inset: Effect of $P_{C_2H_4}$ and catalyst potential on turnover rate of Rh-film catalyst [34]. $P_{O_2} = 1.3$ kPa, $T = 320^\circ\text{C}$.

kinetic behavior depicted in Figs. 2 and 3 suggests that the abrupt rate transition is due to the formation (Fig. 2) or decomposition (Fig. 3) of a surface Rh oxide. The use of the SEP technique has provided strong evidence supporting this idea as discussed in a subsequent section.

Figs. 2 and 3 show a pronounced support effect on the activity of Rh. The highest combustion activities were obtained over Rh/TiO₂ (W⁶⁺) and Rh/ZrO₂ (Y₂O₃) catalysts. The beneficial effect of doping of the TiO₂ carrier with W⁶⁺ cations is also illustrated in these figures. It is also worth noting that the $P_{O_2}^*$ value increases in parallel with increasing catalytic activity (Fig. 2), or, equivalently $P_{C_2H_4}^*$ decreases in parallel with increasing catalytic activity (Fig. 3). The catalysts with higher activity (due to the support) require higher oxygen partial pressures (i.e. oxygen activity) in order to form the surface Rh oxide. Emphasis must also be given to the fact that strong similarities appear between the effect of the supports on the reaction rate behavior (Figs. 2 and 3) and the effect which had been

observed during the NEMCA investigation of this reaction on Rh film catalysts upon varying the catalyst potential, in galvanic cells of the type: C₂H₄, O₂, Rh/YSZ/Pt, air [34]. The latter results are shown as an inset in Figs. 2 and 3, for comparison reasons, and will be discussed below.

A comparison of catalytic activity of Pd supported on the five substrates, at 320°C under C₂H₄ oxidation is illustrated in Figs. 4 and 5. The kinetic curves indicate that the reaction exhibits a Langmuir–Hinshelwood type behavior, with competitive adsorption of C₂H₄ and oxygen (Figs. 4 and 5). The pronounced effect of the supports on the specific activity of Pd catalysts is again obvious. Increased activities were observed upon doping the TiO₂ supports with W⁶⁺ cations, as in the case of Rh metal. Pd/ZrO₂ (8% Y₂O₃) is significantly more active than Pd/γ-Al₂O₃ or Pd/SiO₂ and much more active (180-fold) enhancement than Pd/TiO₂.

In order to examine the possible structure sensitivity of the C₂H₄ oxidation reaction, the effect of the

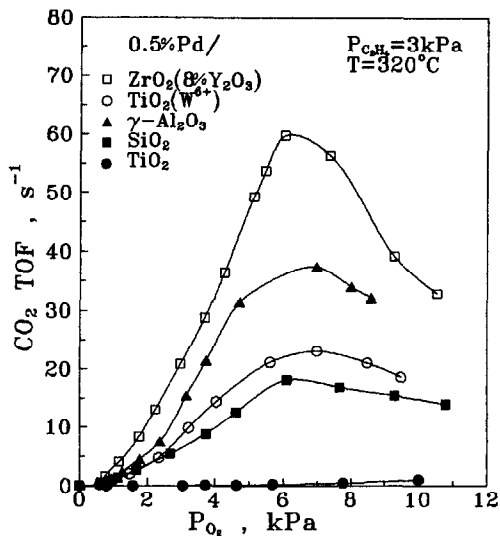


Fig. 4. Effect of partial pressure of oxygen (P_{O_2}) and supports on catalytic turnover rate of Pd catalyst.

average Pd crystallite size of Pd/ γ - Al_2O_3 model catalyst was tested. Fig. 6 shows the turnover frequency of C_2H_4 oxidation as a function of the average Pd crystallite size. The variation of the dispersion of this catalyst was achieved by sintering of the highly-dispersed formulation at different temperatures and time periods. Fig. 6 clearly shows that C_2H_4 oxidation is a facile reaction since its turnover frequency is not affected by Pd dispersion. Thus, the variation of

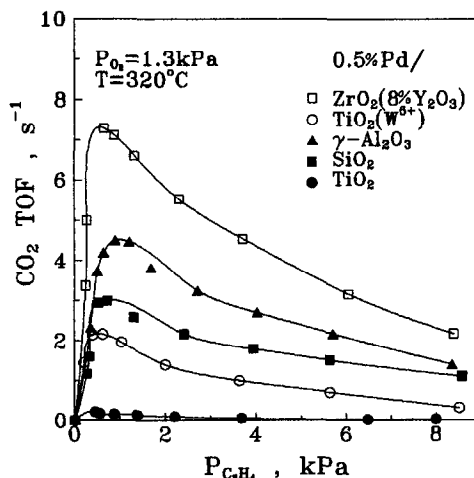


Fig. 5. Effect of partial pressure of ethylene ($P_{C_2H_4}$) and supports on catalytic turnover rate of Pd catalyst.

specific activity with the carrier (Figs. 4 and 5) cannot be related to structure sensitivity considerations and should be attributed to interactions between the metal crystallites and the carrier.

Figs. 7 and 8 illustrate the effects of the support on C_2H_4 oxidation activity of Pt while varying oxygen (Fig. 7) and ethylene (Fig. 8) partial pressures. Significantly enhanced activities were observed for the case of Pt/ ZrO_2 (8% Y_2O_3) catalyst, while the inverse behavior (compared with Rh and Pd metals) was observed upon doping the TiO_2 supports with W^{6+}

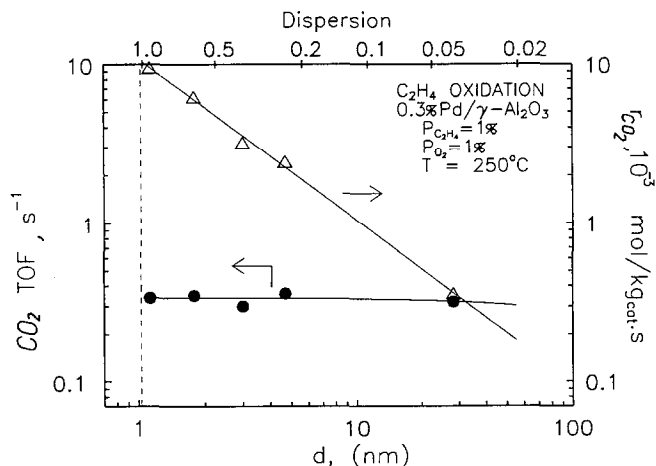


Fig. 6. Effect of catalyst dispersion and crystallite size on the reaction rate and turnover frequency of ethylene oxidation on Pd/ γ - Al_2O_3 .

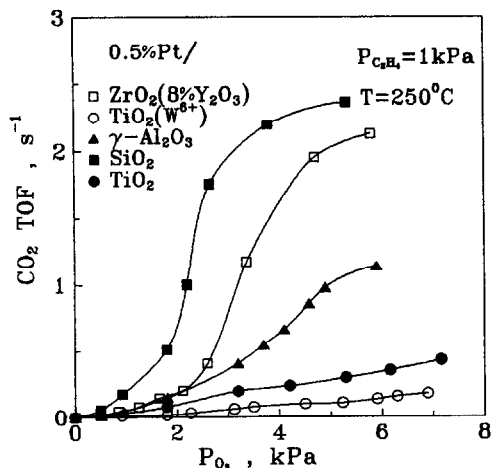


Fig. 7. Effect of partial pressure of oxygen (P_{O_2}) and supports on catalytic turnover rate of Pt catalyst.

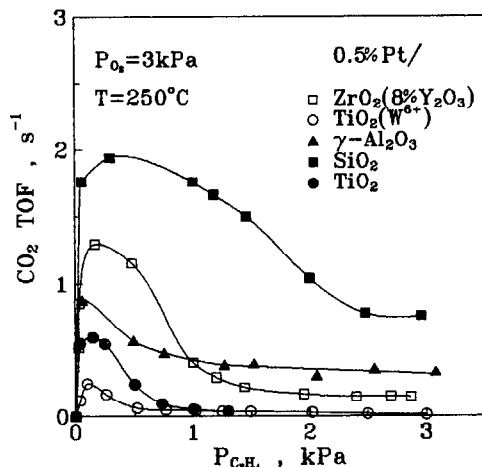


Fig. 8. Effect of partial pressure of ethylene ($P_{C_2H_4}$) and supports on catalytic turnover rate of Pt catalyst.

cations. Pt/SiO₂ exhibited the highest specific activity among the Pt catalysts.

Comparison of the activity results presented above reveals the generally superior activity of Pd-supported catalysts for this reaction (Fig. 9), in agreement with results reported in the literature [12]. The best carriers for the different metals are TiO₂ (W⁶⁺) for Rh, ZrO₂ (Y₂O₃) for Pd and SiO₂ for Pt. These conclusions can be very important for the development of improved automotive exhaust catalytic converters [47].

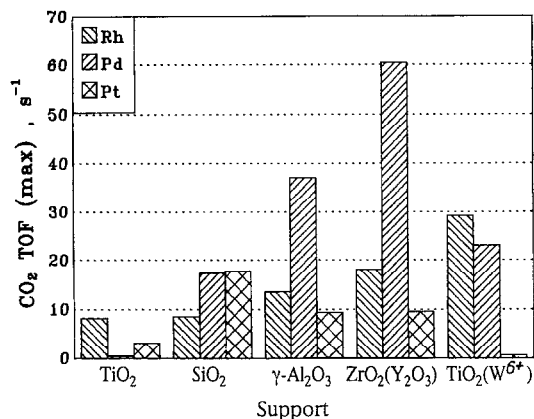


Fig. 9. Comparison of the turnover activity of the fifteen model catalysts investigated for the ethylene oxidation reaction at 320°C

3.3. SEP and NEMCA study of C₂H₄ oxidation on Rh catalyst films

The kinetics of C₂H₄ oxidation were also investigated in detail on Rh catalyst films under open circuit conditions (SEP measurements) in a galvanic-cell reactor or the type: C₂H₄, O₂, Rh/YSZ/Pt, air. The same cell was used for the study of the reaction under closed circuit conditions where the NEMCA effect on the catalytic system was widely investigated [34].

3.3.1. Open-circuit kinetics and potentiometric measurements

The measurement of the open-circuit catalyst potential V_{WR}^0 of a solid electrolyte galvanic cell in which one electrode (working) is also used as a catalyst, can give useful in situ information concerning the thermodynamic activity of oxygen adsorbed on the catalyst–electrode surface, via the Nernst equation [46]:

$$V_{WR}^0 = (RT/4F)\ln(\alpha_0^2/0.21) \quad (1)$$

or, equivalently,

$$\alpha_0 = (0.21)^{1/2}\exp(2FV_{WR}^0/RT) \quad (2)$$

where α_0 is the catalyst surface oxygen activity and 0.21 is the oxygen activity of the reference Pt/air electrode. The above equations are valid only under open-circuit conditions, and the assumptions for their use are discussed in detail elsewhere [43–46]. Thus,

comparison of simultaneously obtained kinetic and potentiometric results can be very useful for studying the mechanism of the catalytic reaction since the potentiometric results provide direct in situ information concerning the activity of oxygen adsorbed on the catalyst during the reaction. In fact, SEP is one of the very few techniques which can be used in situ to extract information concerning adsorbed species on catalyst surfaces without UHV requirements [43,46].

Figs. 10 and 11 show the effect of oxygen (Fig. 10) and ethylene (Fig. 11) partial pressures on the regular open-circuit rate of C_2H_4 oxidation and on the simul-

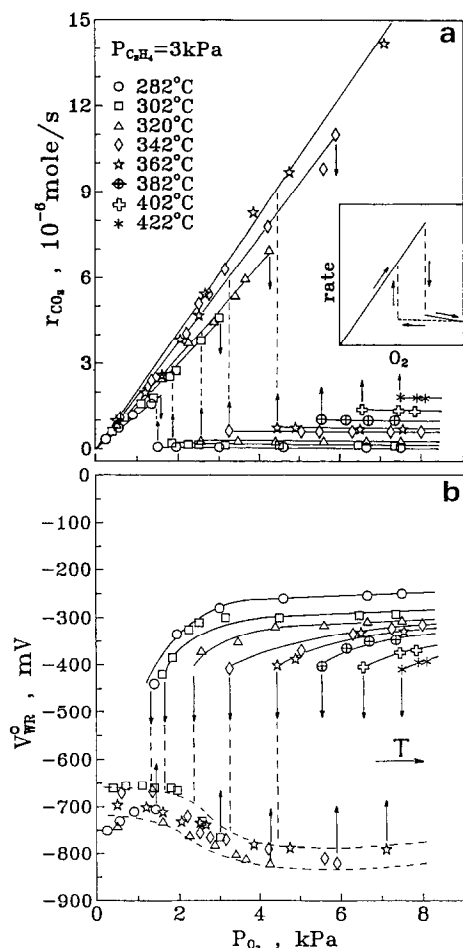


Fig. 10. Effect of partial pressure of oxygen and temperature on the reaction rate (a) and open circuit potential (b) during ethylene oxidation on Rh films supported on YSZ solid electrolyte (see text for discussion).

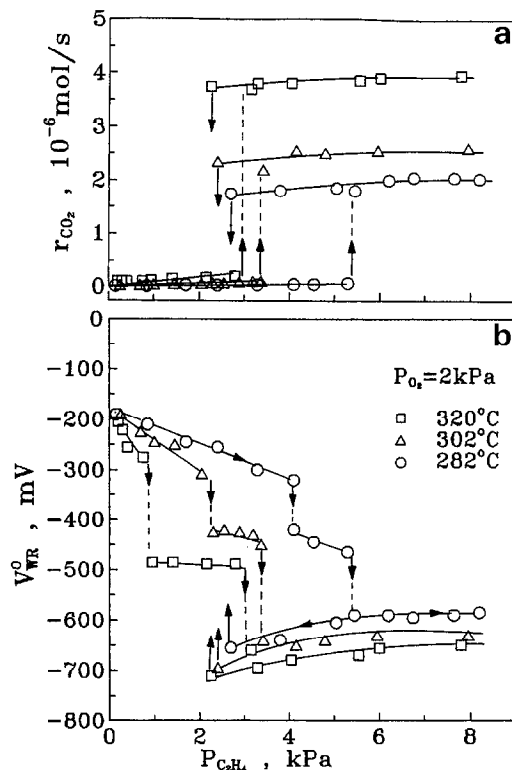


Fig. 11. Effect of partial pressure of ethylene and temperature on the reaction rate (a) and open circuit potential (b) during ethylene oxidation on Rh films supported on YSZ solid electrolyte (see text for discussion).

taneously measured open-circuit catalyst potential, V_{WR}^0 , at constant $P_{C_2H_4}$ and P_{O_2} , respectively. Similar to the kinetic behavior which was observed over the supported Rh catalysts (Figs. 2 and 3), the appearance of critical $P_{O_2}^*$ (Fig. 10) and $P_{C_2H_4}^*$ (Fig. 11) values is obvious. At these critical reactant partial pressure values abrupt rate transitions occur, which are accompanied by a significant, up to 150 mV, shift in V_{WR}^0 . Such shifts in open circuit potential have also been observed experimentally in previous studies of C_2H_4 [44] and CO [45] oxidation on Pt.

The potentiometric results of Fig. 11 indicate a second shift in V_{WR}^0 which is not followed by any rate modification and which is always obtained at lower $P_{C_2H_4}$ values, that is, higher oxygen activity values than those corresponding to the low V_{WR}^0 shift which is accompanied by the abrupt rate transition. This catalyst potential shift may be related to transi-

tion between different surface oxides with similar catalytic properties.

The appearance of a significant hysteresis behavior on the rate while varying P_{O_2} (Fig. 10) or $P_{C_2H_4}$ (Fig. 11) should also be pointed out. Thus, when starting from low oxygen partial pressure (i.e. a pre-reduced catalyst surface) and subsequently increasing P_{O_2} , the reaction rate follows the enhanced activity first-order behavior, until the critical $P_{O_2}^*$ value is reached. At this state, the catalyst surface is oxidized and the reaction rate decreases abruptly. If now the reverse procedure is followed, that is, decreasing P_{O_2} , the rate of the reaction follows a different path, thus defining an hysteresis loop. When an oxygen partial pressure is reached where the surface oxide decomposes, the reaction rate increases again approaching values corresponding to the reduced surface state of the catalyst. However, the oxygen partial pressure at which this transition occurs is lower than $P_{O_2}^*$. The same hysteresis loop is observed by following the opposite clockwise procedure. Analogous hysteresis loops are observed by varying $P_{C_2H_4}$ at constant P_{O_2} (Fig. 11).

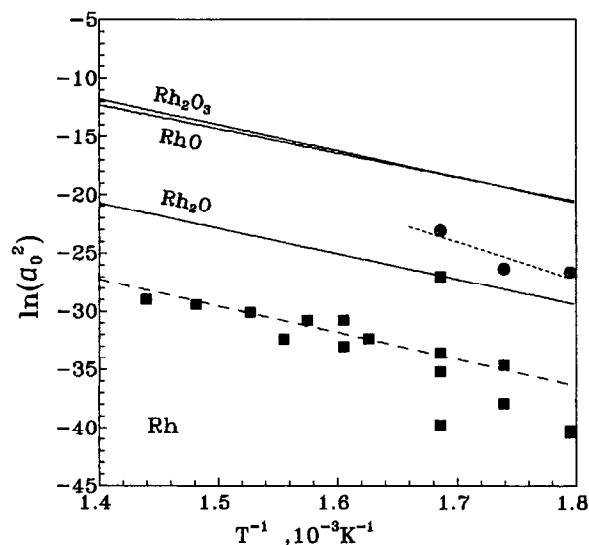


Fig. 12. (■): Temperature effect on the surface oxygen activity of the oxidized surface at the rate transition ($P_{O_2} = P_{O_2}^*$, $P_{C_2H_4} = P_{C_2H_4}^*$) and comparison with the stability limits of bulk Rh oxides. (●): Surface oxygen activity at which a transition to lower α_0 values occurs without any effect on the reaction rate (Fig. 11b, see text for discussion).

Fig. 12 shows the upper limit (oxidized surface) of the catalyst potential and the corresponding oxygen activity, α_0 , at which the abrupt rate transition takes place (dashed line). It is also shown in 12 that the oxygen activity values (dotted line) for which an abrupt shift on the open-circuit potential was observed without being followed by any rate modification (Fig. 11). The solid lines shown on the figure correspond to the stability limits of bulk Rh oxides.

3.3.2. Closed-circuit kinetics. The NEMCA effect

It has been reported [34] that by applying external potentials and thus supplying O^{2-} to the Rh catalyst surface through the YSZ solid electrolyte in galvanic cells described above, up to 100-fold increases in catalytic rates can be obtained for the case of C_2H_4 oxidation. The steady-state rate of oxidation of C_2H_4 over Rh upon varying catalyst potential, is shown as an insert in Figs. 2 and 3 as a function of P_{O_2} and $P_{C_2H_4}$, respectively. Attention is drawn on the similarities of the effects of the supports and the effects of applied potential. Increasing catalyst potential causes similar rate enhancement as variation of the catalyst support in the order: TiO_2 , SiO_2 , $\gamma-Al_2O_3$, ZrO_2 (8% Y_2O_3), TiO_2 (W^{6+}). Since the NEMCA effect is due to alterations in catalyst work function, $e\Phi$, with changing catalyst potential ($\Delta e\Phi = e\Delta V_{WR}$) [32,33] and to the concomitant back-spillover of promoting oxide ions onto the catalyst surface [33,40], it is likely that the observed effects of the support are related to changes in the work function of the supported Rh crystallites, induced by interactions between the metal particles and the carriers. If that is the case, it can be argued that $e\Phi$ is the lowest for Rh supported on TiO_2 and highest for Rh supported on doped TiO_2 (W^{6+}).

4. Discussion

The present results show that supports can play an important role in influencing the activity of three-way automotive exhaust catalysts for the oxidation of light hydrocarbons such as C_2H_4 . The kinetic behavior of C_2H_4 oxidation on supported Rh catalysts (Figs. 2 and 3) clearly indicates the existence of two kinetic regimes: one corresponding to low $P_{O_2}/P_{C_2H_4}$, the other corresponding to high $P_{O_2}/P_{C_2H_4}$ ratio values. The use of the technique of SEP, for the in situ

measurement of the activity of oxygen on the catalyst surface, strongly supports the idea that these two regimes correspond to a reduced and an oxidized catalyst surface, respectively. In fact, the observation that the $\ln\alpha_0^2$ increases linearly with T^{-1} with a slope corresponding to a ΔH of 88 kJ/gatom O, that is, comparable to the value of bulk rhodium oxide formation (Fig. 12), corroborates the assignment of the rate transition to surface oxide formation and the assignment of α_0^2 at which the transition takes place to the stability limit of surface rhodium oxide. The rhodium oxides which can form on the catalyst surface seem to poison the reaction with a similar mechanism, not altering significantly the reaction parameters. As a result the transition between different Rh oxide phases is not accompanied by significant changes of the reaction rate. This is illustrated in Fig. 11b, in which the brakes of the V_{WR}^0 curves at low ethylene pressures are not followed by rate modifications. The formation of several Rh oxide phases on rhodium is well documented both under atmospheric pressure [1,2] and under UHV conditions [48]. The temperature variation of the activity of oxygen at which the low $P_{C_2H_4}$ transition of open-circuit potential take place (Fig. 11b) and which is not followed by any rate transitions, gives a slope corresponding to a ΔH value of approximately 134 kJ/gatom O. The position of this line on the phase diagram (Fig. 12) corroborates the suggestion that it could correspond to surface Rh_2O_3 or RhO phases.

It is apparent from Figs. 10 and 11 that the turnover activity on the reduced catalyst surface is much higher than on the oxidized surface. On the reduced surface the rate is near first order in oxygen, near zero order in C_2H_4 and there is no evidence of competitive adsorption of the reactants. On the other hand, the formation of the surface oxide and the subsequent abrupt decrease of the rate, could possibly prevent the reaction rate from exhibiting a Langmuir–Hinshelwood form, in particular when the rate maxima would appear at oxygen partial pressures higher than those required for the formation of surface oxides. The rate shows a first-order dependence in C_2H_4 and negative order in oxygen on the oxidized surface, indicating competitive adsorption and a predominantly oxygen-covered surface.

It must be noted that the supports not only affect strongly the catalytic activity (Figs. 2 and 3) but also

appear to have a significant effect on $P_{O_2}^*$ and $P_{C_2H_4}^*$ values, that is, on the stability limit of the surface oxide (Figs. 2 and 3). This causes a dramatic (up to two orders of magnitude) enhancement of catalytic activity for intermediate P_{O_2} and $P_{C_2H_4}$ values (Figs. 2 and 3).

The following sequence, in order of decreasing catalytic activity, was observed for Rh catalysts under conditions of ethylene oxidation, at relatively high oxygen pressures: Rh: $TiO_2 (W^{6+}) > ZrO_2 (8\% Y_2O_3) > \gamma-Al_2O_3; SiO_2 > TiO_2$, and it is remarkable that the same sequence applies in terms of the $P_{O_2}^*/P_{C_2H_4}$ or $P_{O_2}/P_{C_2H_4}^*$ value (i.e. oxygen activity) required for the surface oxide formation (Figs. 2 and 3). It should be noted, however, that at low oxygen and high ethylene partial pressures, when the catalysts exists in its reduced state, the activity of Rh/ TiO_2 is very close to that of Rh/ $TiO_2 (W^{6+})$.

A qualitatively similar kinetic behavior was observed over Rh polycrystalline films operating under NEMCA conditions [34] in the electrochemical cell reactor of the type: $C_2H_4, O_2, Rh/YSZ/Pt, Air$. It was observed that increasing catalyst potential and, thus, increasing catalyst work function [32,33,40], caused a large increase in catalytic turnover rate as well as a significant increase in the $P_{O_2}/P_{C_2H_4}$ value required for surface oxide formation (inserts of Figs. 2 and 3). All previous NEMCA studies, involving YSZ as the solid electrolyte [33,40] have been rationalized in terms of the following simple and theoretically well-established rule [33,40]: increasing the V_{WR} and $e\Phi$ of the catalyst surface by supplying back-spillover negative charged ions, $O^{\delta-}$, causes weakening of the chemisorptive bond strength of electron acceptor adsorbates, such as dissociatively chemisorbed oxygen, and strengthening of the chemisorptive bond strength of electron donor adsorbates such as ethylene. Based on this rule we have reported a detailed interpretation of these results [34]. The experimental observations have been explained considering the effects of the externally imposed work function changes on the chemisorption properties of the electron acceptor (oxygen) and electron donor (ethylene) chemisorbed species. Thus, an increase of the catalyst work function causes weakening of the Rh=O bond and strengthening of the Rh- C_2H_4 bond, both consistent with the observed effect on $P_{O_2}^*$ and $P_{C_2H_4}^*$ [34]. In fact, destabilizing the Rh=O bond

implies that higher P_{O_2} values (or, equivalently, higher surface oxygen activities) are required in order to form rhodium oxide (Figs. 2 and 3).

The results of the present study clearly illustrate the strong influence of the catalyst carrier on the relative pressures of oxygen and ethylene as well as temperature which are required to cause transitions in the surface state of rhodium under reaction conditions (i.e. from reduced to oxidized states and vice versa). The similarities between the support effects and the NEMCA effects in this respect may possibly indicate that the two phenomena cause qualitatively similar alterations in the surface state of the metal particles under reaction conditions. Since changes in the surface work function have been observed under NEMCA conditions [33,40], it may be argued that similar changes in the surface work function of the Rh particles occur upon interaction of the metal with the carrier material. In that case, the classification of the carrier materials in the sequence of increasing $P_{O_2}/P_{C_2H_4}$ required to form surface oxides of Rh might also reflect the sequence in the order of decreasing positive difference in work function of the Rh metal, caused by its interaction with the carrier material.

The alteration of the electronic state of the supported Rh particles (changes in work function) may be the result of electronic interactions at the metal–support interface which influence the electronic parameters of the interface metal atoms [20–22]. For very small metal particles (<20 Å) a large fraction of the metal atoms is at or very close to the interphase between the two materials. It has also been estimated [24] that for relatively small metal particles (<100 Å) significant alterations in the work function may be expected when the particles are dispersed on W^{6+} -doped TiO_2 carriers.

Equivalently, it may be suggested that back-spillover of oxygen ions ($O^{\delta-}$) on the surface of the Rh particles, originating from the carrier, may be responsible for the observed alterations in catalytic activity. In fact, supports such as TiO_2 (W^{6+}) and ZrO_2 (8% Y_2O_3), which give the highest turnover rates, are known from the literature [49] to have a significant oxygen storage capacity [49]. Oxygen anions from the solid electrolyte support can easily migrate on the surface of metal crystallites and thus enhance their catalytic activity [33]. The driving force for the back-

spillover of ions is their electrochemical potential and concentration gradient since they can also react, albeit at a slow rate, with C_2H_4 on the metal surface [33,40]. Oxide ions can be regenerated from gaseous oxygen at the three-phase boundaries of other metal crystallites, so that a steady state is maintained.

A similar explanation can be proposed for some of the interesting results of Baiker and coworkers [27–31] concerning the enhanced catalytic properties of supported metal/ ZrO_2 catalysts as well as the results of Metcalfe and Sundaresan [25]. The latter authors have found that Pt supported on YSZ is by a factor of five more active for CO oxidation than Pt supported on Al_2O_3 . The authors have attributed their findings to an enhanced interfacial reaction at the solid electrolyte–metal crystallite–gas three-phase boundaries. This is a reasonable explanation, but the results can also be explained invoking an in situ NEMCA effect.

The existence of significant hysteresis phenomena on the kinetic behavior of ethylene oxidation on Rh (Figs. 10 and 11) when varying the partial pressures of the reactants (i.e. surface oxygen activity) is directly related to the formation/decomposition of the surface Rh oxide. Several heterogeneous catalytic systems operating near the surface oxide stability limit have often been found to exhibit oscillatory behavior. Typical examples are the $C_2H_4/O_2/Pt$ [44] and $CO/O_2/Pt$ [45] systems in which the rate was found to oscillate between two states, one corresponding to the reduced surface and the other corresponding to the oxidized surface states [45]. In both studies, the use of SEP was found very useful for the explanation of the experimental observations [44,45]. Other systems, operating under similar conditions (near the surface oxide stability limit) can exhibit hysteresis phenomena instead of oscillations, as analysed by Rieker [50]. The present system is a typical example of the latter case.

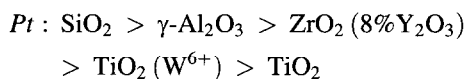
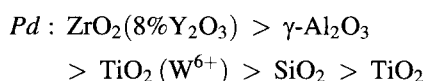
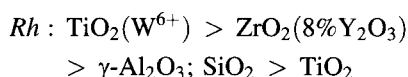
In the case of Pd catalysts (Figs. 5 and 6), similar support induced effects on the turnover rate have been observed and the activity was found to decrease according to the following sequence: Pd: ZrO_2 (8% Y_2O_3) > γ - Al_2O_3 > TiO_2 (W^{6+}) > SiO_2 > TiO_2 . The variation of intrinsic activity with the carrier employed for the dispersion of the Pd particles can be explained using the same arguments as in the case of Rh. Although, the appearance of the superior behavior of γ - Al_2O_3 in comparison with TiO_2 (W^{6+}) is not so clear, the results show enhancement in turnover

frequency caused by supports which might promote the mobility of O^{2-} species, which can backspillover on catalyst surface causing an increase in the work function and thus weakening of the Pd=O bond.

Platinum-supported catalysts have shown drastically different behavior in comparison with that of Rh and Pd. The observed catalytic turnover activity sequence is the following: Pt:SiO₂ > γ -Al₂O₃ > ZrO₂ (8% Y₂O₃) > TiO₂ (W⁶⁺) > TiO₂. Therefore, the apparent 'active' (for the case of Rh or Pd) supports such as W⁶⁺-doped TiO₂ and ZrO₂ appear to be inferior to the apparent 'non-active' supports such as SiO₂ or γ -Al₂O₃. This observation is not new in the literature. It has been found that the chemisorption capacity and activity of Pt is significantly suppressed when it is supported on TiO₂ doped with higher valence cations [19,20,51,52], while the inverse behavior was observed for Rh, which, when supported on higher valence doped TiO₂ exhibits enhanced catalytic activity [23,52,53].

5. Summary and conclusions

1. The rate of oxidation of ethylene can be altered significantly by using different supports for the dispersion of the three metals investigated, namely, Pt, Pd and Rh.
2. The following sequence of catalytic activity was observed:



3. These turnover frequency variations are attributed to interactions between the metal crystallites and the carrier, while explanations invoking structure sensitivity considerations are not supported by experiment.
4. The qualitatively similar results obtained in the NEMCA study of the reaction gives rise to similar explanations for the origin of both effects. Surface

spectroscopic and work function measurements could further elucidate this point.

References

- [1] G.L. Kellogg, Surf. Sci. 171 (1986) 359; J. Catal. 65 (1985) 167.
- [2] S.H. Oh, J.E. Carpenter, J. Catal. 80 (1983) 472.
- [3] S.H. Oh, G.B. Fisher, J.E. Carpenter, D.W. Goodman, J. Catal. 65 (1980) 360.
- [4] S.H. Oh, C.C. Eickel, J. Catal. 128 (1991) 526.
- [5] L.H. Dubois, P.K. Hansma, G.A. Somorjai, J. Catal. 65 (1980) 318.
- [6] C.-T. Kao, G.S. Blackman, M.A. Van Hove, G.A. Somorjai, Surf. Sci. 224 (1989) 77.
- [7] M. Bowker, Q. Guo, R.W. Joyner, Surf. Sci. 280 (1993) 50.
- [8] A.J. Slavin, B.E. Bent, C.-T. Kao, G.A. Somorjai, Surf. Sci. 206 (1988) 129.
- [9] R.J. Levis, L.A. DeLouise, E.J. White, N. Winograd, Surf. Sci. 206 (1990) 124.
- [10] J.T. Kummer, J. Phys. Chem. 90 (1986) 4747.
- [11] K.C. Taylor, Chemtech (1990) 551; Catal. Rev.-Sci. Eng. 35 (4) (1993) 457.
- [12] G.W. Cordonna, M. Kosanovich, E.R. Becker, Platinum Metals Rev. 33(2) (1989) 46.
- [13] J. Barbier Jr.D. Duprez, Appl. Catal. B 4 (1994) 105.
- [14] G.-M. Schwab, Adv. Catal. 27 (1978) 1.
- [15] F. Solymosi, Catal. Rev. 1 (1967) 233.
- [16] S.J. Tauster, S.C. Fung, J. Catal. 55 (1978) 29.
- [17] C.S. Ko, R.J. Gorte, J. Catal. 90 (1984) 59.
- [18] H.R. Sadeghi, V.E. Henrich, J. Catal. 109 (1988) 1.
- [19] E.C. Akubuiro, X.E. Verykios, J. Catal. 103 (1987) 320; 113 (1988) 106.
- [20] F. Solymosi, I. Tombacz, J. Koszta, J. Catal. 95 (1985) 578.
- [21] T. Ioannides, X. E. Verykios, J. Catal. 140 (1993) 353; 143 (1993) 175; 145 (1994) 479.
- [22] T. Ioannides, X.E. Verykios, M. Tsapatsis, C. Economou, J. Catal. 145 (1994) 491.
- [23] M.A. Vannice, C.G. Twu, S.H. Moon, J. Catal. 79 (1983) 70.
- [24] T. Ioannides, X.E. Verykios, J. Catal. 161 (1996) 561.
- [25] I.S. Metcalfe, S. Sundaresan, AIChE J. 34(6) (1988) 1048; 34(6) (1988) 195.
- [26] S.H. Oh, J. Catal. 124 (1990) 477.
- [27] A. Baiker, R. Schlögl, E. Armbruster, H.J. Gruntherodt, J. Catal. 107 (1987) 221.
- [28] A. Baiker, H. Baris, R. Schögl, J. Catal. 108 (1987) 467.
- [29] D. Gasser, A. Baiker, Appl. Catal. 48 (1989) 279.
- [30] A. Baiker, D. Gasser, J. Cenzner, A. Reller, R. Schloögl, J. Catal. 126 (1990) 555.
- [31] A. Baiker, Faraday Discuss., Chem. Soc. 87 (1989) 239.
- [32] C.G. Vayenas, S. Bebelis, S. Ladas, Nature (London) 343 (1990) 625.
- [33] C.G. Vayenas, S. Bebelis, I.V. Yentekakis, H.-G. Lintz, Catal. Today 11 (1992) 303.

- [34] C.A. Pliangos, I.V. Yentekakis, X.E. Verykios, C.G. Vayenas, *J. Catal.* 154 (1995) 124.
- [35] I.V. Yentekakis, G. Moggridge, C.G. Vayenas, R.M. Lambert, *J. Catal.* 146 (1994) 292.
- [36] I.V. Yentekakis, C.G. Vayenas, *J. Catal.* 149 (1994) 238.
- [37] T.I. Pilitova, V.A. Sobyenin, V.D. Belyaev, *React. Kinet. Catal. Lett.* 41 (1990) 321.
- [38] C.A. Pliangos, I.V. Yentekakis, S. Ladas, C.G. Vayenas, *J. Catal.* 159 (1995) 189.
- [39] J. Pritchard, *Nature* 343 (1990) 592.
- [40] C.G. Vayenas, M.M. Jaksic, S. Bebelis, S. Neophytides, in J.O.M. Bockris, B.E. Conway, B.E. White (Eds.), *Modern Aspects of Electrochemistry*, No. 29, Plenum Press, New York, 1996, pp. 57–202.
- [41] S. Neophytides, C.G. Vayenas, *J. Phys. Chem.* 99 (1995) 17063.
- [42] M. Makri, C.G. Vayenas, S. Bebelis, K.H. Besocke, C. Cavalca, *Surf. Sci.* (1996) in press.
- [43] C.G. Vayenas, *Solid state Ionics*, 28–30 (1988) 1521.
- [44] C.G. Vayenas, B. Lee, J.N. Michaels, *J. Catal.* 66 (1980) 36.
- [45] I.V. Yentekakis, S. Neophytides, C.G. Vayenas, *J. Catal.* 111 (1988) 152.
- [46] C. Wagner, *Adv. Catal.* 21 (1970) 323.
- [47] V.G. Papadakis, C.A. Pliangos, I.V. Yentekakis, C.G. Vayenas, X.E. Verykios, *Catal. Today* 29 (1996) 71.
- [48] A.D. Logan, A.K. Datye, J.E. Houston, *Surf. Sci.* 245 (1991) 280.
- [49] E.C. Subbarao, (Ed.), *Solid Electrolytes and their Applications*, Plenum, New York, 1980.
- [50] H. Rickert, *Angew. Chem., Int. Engl.*, Ed. 17 (1978) 37.
- [51] E.C. Akubuiro, X.E. Verykios, T. Ioannides, *Appl. Catal.* 46 (1989) 297.
- [52] E.C. Akubuiro, T. Ioannides, X.E. Verykios, *J. Catal.* 116 (1989) 590.
- [53] Z. Zhang, A. Kladi, X.E. Verykios, *J. Catal.* 148 (1994) 732.